Journal of Environmental Chemical Engineering 10 (2022) 107025

Contents lists available at ScienceDirect

Journal of Environmental Chemical Engineering

journal homepage: www.elsevier.com/locate/jece

Study of amine customized exfoliated BN sheets in SPEEK-PES based blend membrane for acid-base cation exchange membrane fuel cells

Raja Pugalenthi M [a], Gayathri R [a], Guozhong Cao [b], Ramesh Prabhu M [a,*]

[a] Department of Physics, Alagappa University, Karaikudi 630003, TamilNadu, India
[b] Department of Materials Science and Engineering, University of Washington, Seattle, WA 98195-2120, United States

ARTICLE INFO

Editor: Despo Kassinos

Keywords:
Sulfonated poly ether ether ketone
Poly ether sulfone
Boron nitride
Conductivity
Fuel cell

ABSTRACT

The cation exchange membrane is fabricated by assemble of synthetic acid–base pairs in the composite matrix. Polydopamine modified boron nitride (AH-BN) sheets are syntheses that contain the base groups (–NH_2 and –NH–) and incorporated into the sulfonated poly ether ether ketone (SPEEK)-poly ether sulfone (PES) matrices for fabricate the composite membranes. The exfoliated AH-BN sheets are evenly dispersed and strongly interacted with the SPEEK via electrostatic interplay, which modify the nanophase structure and enhance the chain packing of the composite membranes. Adding of 3 wt% AH-BN into the SPEEK-PES exhibits the elevated conductivity of 79.8 mS cm^{-1} and power density of 131.1 mW cm^{-2} at 80 °C under low humidification (50%RH) that is higher compared to the SPEEK (21.2 mS cm^{-1} and 74.2 mA cm^{-2}). The acid–base pairs are created at SPEEK-PES and AH-BN interfaces offers continues pathway channels for the transport of protons with minimum energy barrier via Grotthuss mechanism. Besides, it shows the power density of 172 mW cm^{-2} at 80 °C under 75%RH, which is higher than Nafion 117 (142 mW cm^{-2}). The high residual weight of 93.34% at 170 °C and 97.12% is obtained after TGA and Fenton study. Accelerated stability test (AST) shows the excellent voltage retention about 0.05 V after the 80 h of test that confirm the excellent chemical stability from radical effect.

1. Introduction

The fuel cell is the effective power conversion device with high efficiency and eco-friendly environmental which is the effective solution for the energy crises, exhaustion of the fossil fuel and emission of harmful gases. Hydrogen (H_2) has the possible source of future fuel, reduces the dependent on fossil fuel, and diminishes the pollutant from the industry. It contains the high specific energy, energy yield (122 kJ g^{-1}) and energy per unit mass significantly creates the favorable condition for the fuel cells. The most remarkable benefit is an environmentally friendly since it emits only water by product when employed in a fuel cell. Thus, it achieved the limited efficiency and low catalytic reaction, and problems of hydrogen storage capability because it requires ~4 and 19 times more volume storage than gasoline as liquid and gas states [52–54]. The separation of gas mixtures is a key factor for the energy sector and is necessary for the efficient improvement of biogas and natural gas [55,56]. The hydrogen fuel cell contains the partially-permeable membrane that hinders the other species and intended to allow protons (H^+). The benefits of the proton exchange membrane fuel cell (PEMFC) are high efficiency factor, environmentally friendly and the abundant source of fuel [1,2]. The Nafion (fluorinated) is a trademark membrane for the polymer electrolyte due to inherent thermo-mechanical strength and the high conductive nature. The poor water uptake and lesser mechanical stability causes the poor electrochemical performance at high temperature (>80 °C) and high manufacturing cost controlled the commercialization of Nafion [3,4].

Many polymer were broadly investigated in the PEM such as sulfonated poly ether ether ketone (SPEEK) [5], sulfonated poly ether sulfone [6], poly benzimidazole [7] sulfonated poly phenylene ether ether sulfone, etc [8]. The SPEEK have the remarkable properties likes' low cost, good conductivity and lesser fuel crossover causes the gained interest instead of Nafion. The smaller hydrophilic/hydrophobic separations of SPEEK matrix trigger the high fuel barrier and limited the conductivity, whereas the aromatic back bone provides the high chemical and thermal stability. At higher sulfonation, the SPEEK membrane exhibits the excessive swelling in high temperature which created the strain on the membrane and reduces the MEA stability [9,10]. The problem was rectified in the SPEEK nanocomposite membrane by simultaneous incorporated the polymers and the inorganic additives into SPEEK. In this approach, we fabricates the efficient fuel cell electrolyte with

* Corresponding author.
E-mail address: mkram83@gmail.com (R.P. M).

https://doi.org/10.1016/j.jece.2021.107025
Received 28 October 2021; Received in revised form 27 November 2021; Accepted 15 December 2021
Available online 21 December 2021

enhanced thermo-mechanical stability and proton conductivity of SPEEK [11,26,42]. The blending of SPEEK with the other polymers may reduce the conductivity sites of polymer matrix and enhances the polymer chains stability due to the formation of the ionic/covalent bonds between the polymers via the polar functional groups. These will affect the proton transport channels and made difficult to transport the protons in the polymer matrix, however it restricted the dimensional swelling and favorable condition for the sustainable cell performance [13,26,44].

Poly ether sulfone (PES) is an engineered thermoplastic polymer with outstanding mechanical properties, chemical stability and high transition temperature (Tg, 230 °C), was selected to fabricated SPEEK-PES blend membrane by polymer blending technique [6]. The SPEEK-PES membrane demonstrates the excellent mechanical and thermal properties which is desirable for the durable PEMFC operation. Besides, the pore less microstructure and good film forming capacity was induced in the SPEEK-PES membrane due to identical polymers structure construct good miscibility through the interaction between the SPEEK and PES via sulfonic acid and sulfone groups [44]. Wu reported that by adding 20 wt% PES into the SPEEK the water uptake and proton conductivity at 80 °C was decreases about ~275% and ~15%, respectively. [16]. In contrast, the incorporation of the sufficient amount of nanofillers into the polymer matrix increases the conductivity and the thermo-mechanical stability due its strong synergistic interplay with the water molecules and its polymer chains. At specific weight percentage, the blocking effect was observed in the polymer matrix due to the poor dispersion ability of nanofillers, which block the ionic movement in the polymer channels. Further it will increase the swelling ratio of the membrane owing to the hydrophilic nanofillers drag the more water uptake into the polymer matrix. This phenomenon was observed in the SPEEK composite matrix by incorporating the nanofillers likes zeolites, clay materials and perovkites nanofillers such as $La_2Zr_2O_7$, $BaCeO_3$, Fe_2TiO_5, $SrTiO_3$ [11–13,26,57–60]. To solve this problems through modifying the nanofillers surface (silica, GO and CNT) with the organic groups (acid or base groups) for achieve the even dispersion of the nanofillers within the polymer matrix and induced the strong synergistic contact between the nanofillers and polymer matrix [10,14,15,24]. Especially, amine (base) coated nanofillers are more effective approach than other acids groups because it is favorable for the restriction of water uptake capacity and prevents the dimensional swelling at high temperature [15,61,62]. The transports of the protons mainly occurred between the acid (–S–O^-)-base (-NH_2/–NH-) pairs inform proton donor and acceptors via Grotthuss mechanism, which aids the facile protons migrations with lesser potential barrier operates in high temperature at low humidity condition [63–65]. Hexagonal boron nitride (BN) is the two dimensional (2D) material contains the boron and nitrogen atoms arranged in the hexagonal structure and electrons sharing of this material are similar to the graphite materials. The BN layers sheet are stacked via weak Vander Waals force with distance of 0.333 nm, whereas graphite is held together with distance of 0.335 nm. The mechanically exfoliated BN sheets were produced the proton conductivity in the direction of hexagonal rings is 100 mS cm^{-1} and between the layers of Vander Waals gaps is 0.008 S cm^{-1}. Seong et.al measured the protons conductivity of 100 mS cm^{-1} at the hexagonal rings of BN in the room temperature, which is higher than the conductivity of graphite material (5 mS cm^{-1}) as it contain covalent bonding between the B and N atoms owing to the more electro negativity of the N atoms, which causes to buildup the valence electrons around the N atom and created an irregular distribution of electron cloud [19]. Hu et.al shows that BN based membrane blocks the higher radii ionic particles but transfer only the protons at the center of the sheets through the hexagonal rings [20]. Hu et al. prove that BN is an outstanding conductor of protons (H^+) at room temperature and performing better than that of graphene at elevated temperature. BN shows a rapid rate of increase in an Arrhenius type plot with raises in temperature as compared to graphene material [66]. BN contains the uniqueness over these carbon related materials. The black colors of carbon related materials make the polymer composites membrane as opaque, whereas BN composites membrane are transparent, which infer that the composites can be obtained as desired color. In addition to this, BN has been become high thermo-mechanically stable and maintain the dielectric property of the composite, which are vanished by using the carbon related materials owing to the insulating behavior [67]. The BN contains useful property same as graphene materials such as enhanced surface area, low density, high oxidation resistance, high mechanical and chemical stability, which significantly changes the properties of the composite membrane via effective synergy mechanism between polymer and BN [17,18,25]. The BN was used as the effective filler in the polymer membrane; however aggregation effect was induced by the Vander Waals force which causes the poor dispersion and leading to the weak compatibility with polymer matrices [21]. The drawback in the BN sheets was eliminated by functionalized the various organic materials (amine, sulfonic acids and hydroxyl) via covalent bond without altering any instinct properties [17,22–24]. The poly dopamine is the flexible lower molecular weight materials and easily anchored on the BN surfaces at π-π planar site through condensation reaction [23,24]. The accumulation of acid (–S–O^-)-base (-NH_2/–NH-) pairs induces the strong interfacial interaction between the polymer and 2D sheets construct the proton transport pathways channels and completely modified the polymer stability. The polydopamine were adsorbed on the BN surface via covalent bond, which helps to operate stable and continuous transport of the protons at high temperature with low humidified condition [17].

In this study, the SPEEK is prepared and blended with the PES (20 wt %) to fabricate the SPEEK-PES blend membrane. Further, the poly dopamine modified hexagonal boron nitride (AH-BN) are prepared and incorporated (1.5–4.5 wt%) into the SPEEK (80 wt%)-PES (20 wt%) matrix. The thermal and mechanical stability of the AH-BN sheets are transferred into the SPEEK-PES membrane through the effective synergy interaction between the SPEEK and AH-BN. This reinforcement tends to increases the polymer stability and decreases the dimensional swelling (swelling ratio). The functional groups of amine and hydroxyl are successfully anchored on the AH-BN surface facilitate the superior acid-base proton transfer mechanism through the Grotthuss type that made the superior properties as compared to SPEEK.

2. Experimental

2.1. Materials

The powder form of PEEK (M_w = 20,800 g mol^{-1}) and PES (M_w = 3000 g mol^{-1}) polymer was purchased from the Krishna polymer, India. The hexagonal boron nitride (1 μm) particles, polydopamine hydrochloride (99%) and HCl (98%) were brought from Sigma Aldrich, India. The N,N-dimethylacetamide (DMAc), ethanol, De-ionized water (DD) and the sulfuric acid (98%) were received from Sisco Research Limited (SRL), India.

2.2. Preparation of SPEEK and functionalized hexagonal boron nitride (AH-BN)

The direct sulfonation process is used to prepare the SPEEK, which is briefly stated in the previous work and calculated DS level is 65.15% through the NMR technique [26]. The AH-BN is prepared by simultaneous carry out the exfoliation and hydroxylation process with the BN particles (1 μm) and functionalized by polydopamine groups via condensation process. The exfoliation and hydroxylation are carried out in the BN sheets (450 mg) by immersing in the 75 mL of hydrogen peroxide after the 2 h of sonication. The solution is transferred into the autoclave and maintained at 90 °C for 15 h. The exfoliated BN sheets are separated by centrifuge process for 30 min at 3000 rpm to eliminate the bulk sheets. The obtained H-BN (50–55%) are washed several times with the DD water and dried at 85 °C for 4 h [27]. The AH-BN sheets are

produced by adding the H-BN sheets (100 mg) in the 100 mL of water and poly dopamine (2 mg mL^{-1}) solution then magnetically stirred for 7 h at 90 °C. This process initiates the hydrolysis and condensation reaction between the poly dopamine and hydroxyl groups of H-BN sheets. The centrifuge process separated the AH-BN sheets and washed with the ethanol after dried at 90 °C to obtain the brown colored AH-BN sheets (Scheme1). The photography images are shown in Fig.S1, which concluded the poly dopamine are attached on the H-BN and utilized in the composite membrane.

2.3. Preparation of composite membrane

The 80 wt% SPEEK is dissolved in the 7 mL of DMAc solvent then 20 wt% PES is mixed together to make the blend solution. After various amount of AH-BN sheets (1.5, 3 and 4.5 wt%) are added into the 3 mL of DMAc and stirred for 1 h with ultrasonication. These solutions are added to the blend polymer solution to make the composite polymer solution and continued stirring for 24 h at 30 °C. The composite solutions are poured on the petri dish to evaporate the solvent by heating at 80 °C. The 1.5, 3 and 4.5 wt% AH-BN in the SPEEK (80 wt%)-PES (20 wt%) is named as SR1, SR2 and SR3. The SPEEK (100 wt%) and SPEEK (80 wt %)-PES (20 wt%) is coded as SPEEK and SR0. The photography images of the membranes are shown in Fig.S1. The thicknesses of the membranes are in the ranges from 80 to 95 ± 2 μm.

2.4. Characterization

The XRD study of the BN, H-BN, AH-BN and the polymer membranes were carried out through the Pro PAnalytic instrument using the CuKα radiation (λ = 0.154 nm) with the scan rate of 10° to 80°. The FTIR study of the BN, H-BN, AH-BN and the polymer membranes were carried out by the Perkin Elmer/Spectrum 2 instrument in the region of 4000–400 cm^{-1} with the resolution of 4 cm^{-1}. The Raman spectroscopy was used to analyzed the defect sites of BN, H-BN and AH-BN by using RFS27 Bruker device utilized the Nd: YAG laser (λ = 1064 nm). The morphology and the elemental mapping of BN, AH-BN and the polymer membranes were examined via FESEM with EDAX techniques using the Supra55 Zeiss instrument working at the vacuum condition. Before the analysis all the dry samples are coated with gold to reduce the charging problems and obtained the clear images. High resolution transmission electron microscope (HRTEM) images of the AH-BN were observed on the Tecnai-20 G2 instrument operated at 200 kV under the vacuum condition. The surface roughness parameters of the polymer membranes were measured by AFM technique (Pico SPM Picoscan 2100, USA) under the contact mode condition. The XPS technique was used to analysis the binding energy and elemental concentration of the AH-BN which was recorded by ESCALAB 250xi instrument through the monochromatic source of Al Kα. The thermal stability of the polymer membranes were analyzed by TGA techniques using the Discovery SDT-650 Simultaneous DSC-TGA instrument between the temperatures from 30 °C to 700 °C at heating rate of 5 °C min^{-1} under desired nitrogen flow. The glass transition temperature was measured by DSC using the same TGA instrument between 30 °C to 400 °C. Mechanical property of the polymer membranes (1.0 cm × 5.0 cm) were studied through the mechanical tester (INSTRON 3365) in the dry state at room temperature by the longitudinal stretching of 2.5 mm min^{-1} with the applied force of 1 kN. This experiment was repeated three times to measure the average value of mechanical properties.

2.4.1. Oxidative stability

The oxidative stability of the polymer membranes were calibrated by change in the weight of the membranes (2 cm × 2 cm) between before and after the Fenton study. Prior to study, the polymer membranes were dried in an oven for 12 h at 85 °C. The weight of dehydrated membranes (W_A) were found and dipped in the Fenton solution (2 ppm of $FeSO_4$ and 3% of H_2O_2) for 5 h at room temperature. Finally, the remaining weight (W_B) and the degradation time of the membranes were calculated. The experiment was repeated three times to measure the average value.

2.4.2. Ion exchange capacity, hydration number and hydrolytic stability

The acid-base titration was used to estimate the ion exchange capacity (IEC) of the polymer membranes. First, measure the weight of the dehydrated membranes (W_d, g) afterward the membranes (2 cm × 2 cm) were immersed in the 1 M NaCl solution to release the H^+ ions and exchange with the Na^+ ions. Later, 0.1 M of NaOH solution was prepared and titrated with the released H^+ ions in the NaCl solution using phenolphthalein indicator. The consumed volume of NaOH during the titration was calculated. The measurement was repetitive for several times to estimate the average IEC values using the equation (1). The hydrolytic stability is the crucial one for the cell performance and

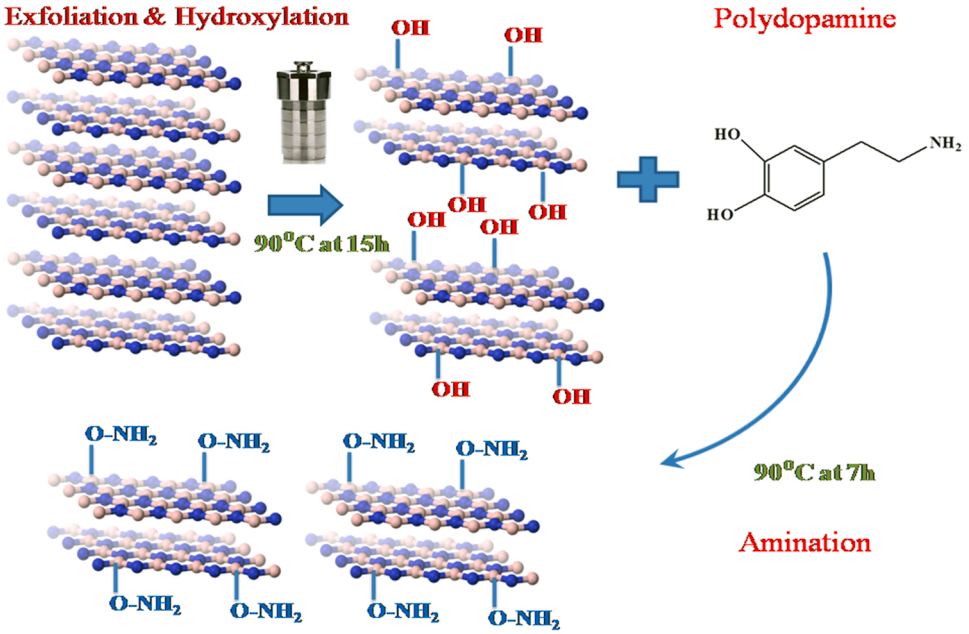

Scheme1. Preparation of AH-BN material.

durability. At first, the membranes (2 cm × 2 cm) were dried in an oven then soaked in the de-ionized water (DD) for 24 h at room temperature. Finally the weight loss was calculated by measuring the weight difference between the after and before immersion. The experiment was repeated three times to measure the average value.

$$\mathrm{IEC} = \frac{\text{consumed NaOH(ml)} \times \text{concentration of NaOH(N)}}{\text{dry weight of samples(g)}} \text{meq g}^{-1} \quad (1)$$

The hydration number calculates the number of bound water molecules attached to the sulfonic acids

$$\lambda = \left(\frac{\text{water uptake value}}{18.01}\right)\left(\frac{10}{\text{measured ion exchange value}}\right) \quad (2)$$

2.4.3. Water uptake and swelling ratio

The water uptake (weight) and the swelling ratio (thickness) of the polymer membranes were calibrated by changes in the weight and thickness of the dry and the wet membranes. Earlier to measurement, polymer membranes were dried in an oven for 15 h at 80 °C. The weight (W_d, g) and thickness (A_d, cm) of dehydrated membranes were calculated afterwards the samples were dipped in the DD water for 24 h at 40, 60 and 80 °C, respectively. The water molecule on the membranes surface was removed by the tissue papers and calculated the weight (W_w, g) and the thickness (A_w, cm) of the membranes. The readings were carried out in several times to check the repeatability of the data. Finally weight and thickness change was calculated by applied the obtained values in the below equations (3) & (4).

$$\text{Weight change} = \frac{(\mathrm{Ww}) - (\mathrm{Wd})}{(\mathrm{Wd})} \times 100 \quad (3)$$

$$\text{Thickness change} = \frac{(\mathrm{Aw}) - (\mathrm{Ad})}{(\mathrm{Ad})} \times 100 \quad (4)$$

2.4.4. Proton conductivity

Proton conductivity of the membranes was measured via conductivity cell through the four probe impedance spectroscopy technique. The resistances of the prepared membranes (diameter 20 mm) were investigated by the frequency response analyzer (μ-Auto lab) with an AC voltage of 10 mV applied in the frequency range from 10 MHz to 10 Hz. The conductivity was measured within the two metal electrodes (20 × 2 mm^2) f—rom the temperatures 30–80 °C at hydrated state of 50%. Before testing, the polymer membranes were immersed in the water for 48 h. Proton conductivity (mS cm^{-1}) of the membranes was calculated via Eq. (5): The experiment was repeated three times to measure the average value.

$$\sigma = \frac{t}{RA} \quad (\text{mS cm}^{-1}) \quad (5)$$

Where t, R, A were thickness, bulk resistance and area of membranes, respectively.

2.4.5. Single PEMFC performances and durability

The PEMFC performance of the membranes was studied by single cell test condition. The membrane electrode assembly (MEA) with an active cell area (5 cm^2) was prepared via hot pressing technique at 125 °C and 3.5 MPa for 1.5 min. The Pt catalyst is the active material with addition to the Nafion (binder) and isopropanol (solvent) were mixed and loaded on the anode and cathode side of the membranes at the rate of 0.20 mg cm^{-2}. The prepared MEA was sandwiched between the two bipolar graphite plates containing the serpentine flow channels. The single cell setup was operated at 80 °C then fed with the hydrogen and oxygen gas in the fixed flow rates of 100 and 200 mL min^{-1}, respectively. Prior to the measurement, the single cell (Bio-Logic VMP-3) was activated with the hydrogen gas and maintained the different humidified temperatures (50 °C and 75 °C). The cell was kept this operating condition for 3 h earlier to measurement of the performance study and perform some cycles at elevated power density. The durability of best performed composite membrane was study by examine OCV degradation via conducting the accelerated stability test at 80 °C in 75% RH for 80 h with required flow of hydrogen (100 mL min^{-1}) and oxygen gas (200 mL min^{-1}) to anode and cathode, respectively.

3. Results and discussion

3.1. XRD

Fig. 1(a)&(b) represent the XRD pattern of BN, H-BN, AH-BN and the prepared membranes. As shown in Fig. 1(a), the AH-BN exhibits the high intense diffraction peaks (2Θ) at 26.66 (002), 41.66 (100) and 54.91 (004) as compared to bulk BN due to the presence of polar groups (OH and NH_2) at the edges of AH-BN sheets. This induces the restacking and disorientation of the sheets, which modify the scattering parameters and produced the high intensity peaks [28]. The sulfonated PEEK reveals the less intense peak (19.5º) than that of SR0 membrane owing to the formation of hydrogen bond between the SPEEK ($\cdots{}^{+}$H-O-S-) and PES (–S═$O^{-}\cdots$) via sulfonic acids and sulfone groups (Fig. 1(b)) [16]. The incorporation of AH-BN sheets (3 wt%) in the SR2 membrane created the strong acid-base interfacial force between the SPEEK (HSO_3) and AH-BN sheets (H–HN–, $^{+}$H–N–), which disorder the crystalline domains and offered the continuous pathways channels for proton transport [24]. The 3 wt% AH-BN (3 wt%) facilitate the enhanced compatibility with the SPEEK matrix due to the good dispersion ability, which likely decreases the peaks intensity of SR2 as compared to SR3 membrane. Thus, 4.5 wt% AH-BN exhibits the aggregation effects results from the bad interfacial interplays with the SPEEK matrix (Fig. 1(b)).

3.2. FTIR

Fig. 2(a)&(b) represents the FTIR spectra of BN, H-BN, AH-BN, SPEEK and their composite membranes. The in-plane and out-plane vibrations of B-N-B bond are occurred at 1348 and 782 cm^{-1} in the BN sheets. The broad and new peaks are observed at 3463 cm^{-1}, 1238 cm^{-1} and 1020 cm^{-1} assigned to O-H, B-OH and B-O vibrations of H-BN, which shows the formation of H-BN from the bulk BN (Fig. 2(a)) [18, 29]. The new peaks are observed at 1276 and 1355 cm^{-1} correspond to the C-C and a C-OH bond that confirms the successful attachment of polydopamine on the AH-BN. The NH_2 and N-H vibration reveals the new peaks at 1651 cm^{-1} and 947 cm^{-1} indicating the anchoring of functional groups at the edges of H-BN surface (π- π electron site) [23, 24]. The symmetric and asymmetric vibration of O═S═O (sulfone groups) in the SPEEK exhibits the absorbance peaks at 1232 and 1088 cm^{-1} correspond to the successful sulfonation. Fig. 2(b) shows the two characteristic peaks at 1009 cm^{-1} and 3400 cm^{-1} in the SPEEK are assigned to the stretching vibrations of S═O and OH groups [16]. The physical interaction between the SPEEK and AH-BN induced the bridging of functional groups via hydrogen interplay ($^{+}$H-O-S- and $^{+}$H–HN–) and decreases the peak intensity at 3400 cm^{-1} as compared to the SPEEK [16,24]. The interactions reveal the best compatibility between the SPEEK and PES with the AH-BN sheets.

3.3. Raman

Raman spectra of BN, H-BN and AH-BN are shown in Fig. S2. This provided the detailed structural fingerprint of B—N, NB—OH and NB—NH bond. The peak at 1366 cm^{-1} was assigned to B-N bond of bulk boron nitride and it's analogous to G band ($E_{2\,g}$ mode) of graphene material. After the exfoliation and functionalization of BN causes the shorting of B-N bond owing to the absent of interlayer interaction, whereas bulk BN produced the elongation of B-N bond [30]. As results, the decreasing and shifting of the peak patterns from 1366 cm^{-1} to 1352 cm^{-1} (blue shift) is observed that is corresponds to the $E_{2\,g}$ phonon

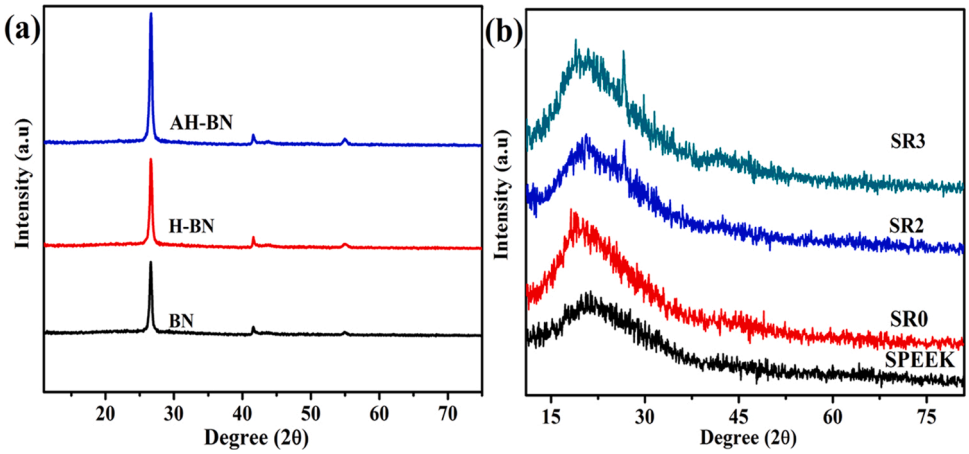

Fig. 1. XRD patterns of (a) BN, AH-BN and (b) SPEEK, SR0, SR2 and SR3 membrane.

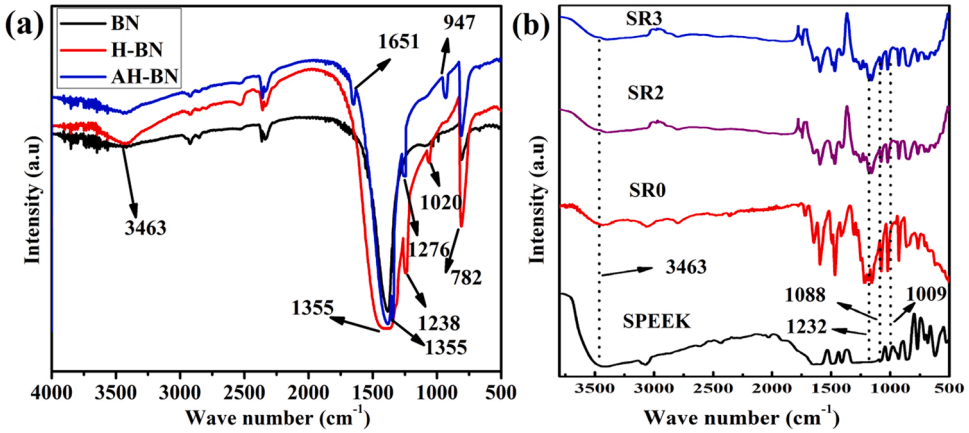

Fig. 2. FTIR patterns of (a) BN, AH-BN and (b) SPEEK, SR0, SR2 and SR3 membranes.

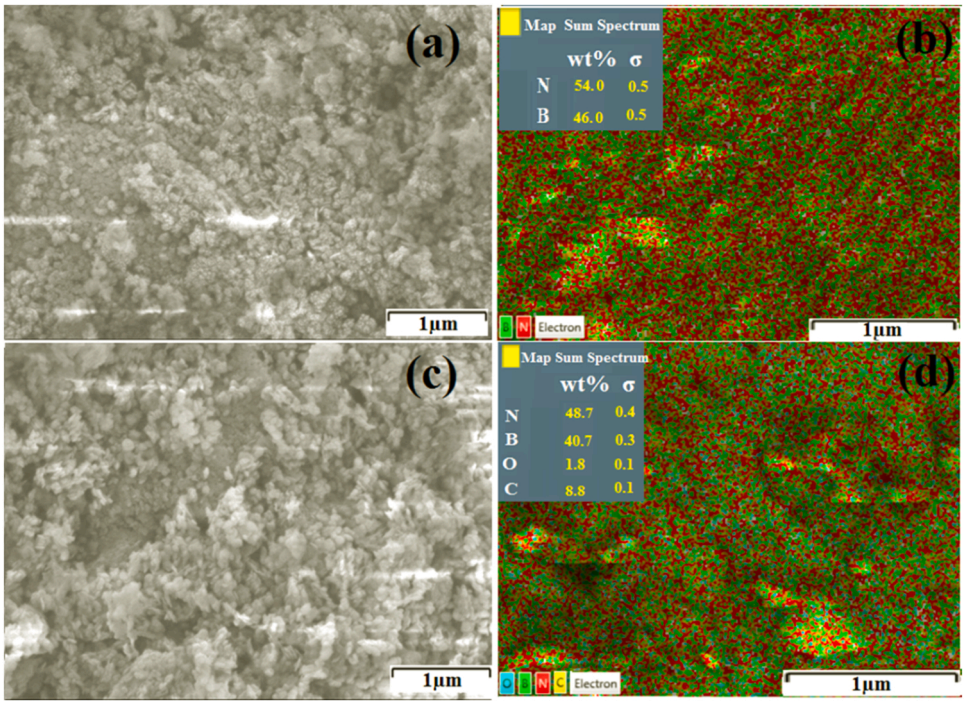

Fig. 3. FESEM image of (a) BN, (c) AH-BN and EDAX mapping image of (b) BN, (d) AH-BN.

mode. The difference in the frequency of the phonon mode attributes the formation of few layered BN sheets (Fig.S2).

3.4. FE-SEM

The FE-SEM was used to study the structural morphology of BN, AH-BN and the composite membrane. The elemental mapping technique was used to study the functionalization and the distribution of AH-BN in the composite membranes. Fig. 3(a)&(c) shows the surface morphology of BN with more stacking of sheets and the AH-BN with lesser stacking of sheets due to effect of the functionalization of BN.

The functionalization reduces the interfacial interplay between the layers due to the presence of amine and hydroxyl on the AH-BN which tend to diminish the aggregation effect of AH-BN sheets [28]. The EDAX and elemental mapping images infers the formation of AH-BN from the bulk BN through chemical process (Fig. 3(b)&(d) and Fig.S3(a–b)& (A–D)). The surface and elemental mapping images of the SPEEK, SR0 and the composite membranes are shown in Fig. 4(a)–(d)&(A)–(D), which reveals the smooth morphology with no obvious cracks on the surface and the distribution of AH-BN on the composite membranes. The incorporation of PES and AH-BN into the SPEEK created the strong interaction between PES/AH-BN and SPEEK via S═O/NH_2 and HSO_3 that rearranged the polymer domains and produced the rigid micro-structure [28]. Embedded AH-BN sheets are well interconnected and dispersed evenly throughout the cross-section regions of SR2 and SR3 membrane; ability to make continuous pathways.

The presence of amines and hydroxyl (–NH_2 and –OH–) on AH-BN sheets minimized the Van der Waals attractive force and increases the strong electrostatic attraction with SPEEK that make smaller the polymer micro-phase separation. Consequently, fractured cross sectional surface of SR2 and SR3 membrane becomes smooth, without pinholes or any cracks (Fig.S4 (a)–(c)) [31]. The cross sectional mapping image of the SR2 membrane shows the good dispersion of AH-BN sheets in the cross sectional matrix than SR3 membrane due to minimize the aggregation of AH-BN and increased interplay with SPEEK (Fig.S5 (a)–(e) & (A)–(E)). As a result, better dispersion was obtained by 3 wt% AH-BN in the SR2 as compared to the 4.5 wt% in the SR3 membrane, which is easily observed from the elemental mapping results.

3.5. AFM

The stability and the proton conductivity of the membranes are much related to the micro structural and morphology property. Fig. 5 shows the 3D and 2D AFM images of SPEEK and composite membranes. The dark and bright segments correspond to the soft and hard regions, which are associated to the hydrophilic and hydrophobic sites. Fig. 5(a)&(A) display the 3D and 2D image of SPEEK reveals the interconnected hydrophilic clusters (dark) due to the presence of more number of sulfonic acids. But, SR0 membrane possesses more hydrophobic sites (bright) due to the attachment of hydrophobic PES to the SPEEK backbone through the ionic interaction of sulfone with sulfonic acids (Fig. 5(b) & (B)). These inhibit the occupation of hydrophilic clusters within polymer matrix and decreases the surface roughness value (R_z) from the 20.1–18.3 nm. The SR2 membrane exhibits the rough surfaces corresponds to the interconnected hydrophilic domains spread throughout the polymer matrices in the effects of the incorporated AH-BN dispersed homogeneously due to 2D structure (Fig. 5(c)&(C)). Besides, bearing of hydroxyl groups at surfaces of AH-BN sheets adsorb the more water molecules and created the continuous ionic pathway channels. These makes the higher thickness of SR2 membrane (70.1 nm) as compared to the SR3 (37.5 nm) owing to the aggregation effect of 4.5 wt% AH-BN sheets, which significantly decreases the roughness value of SR3 membrane (Fig. 5(c–d) & (C–D)) (Table1) [32,33].

3.6. TEM

The TEM image of AH-BN sheets is shown in Fig. 6(a), which shows the 2D morphology of BN is still maintained after the functionalization and establish layered sheets like structure. The low transparency (dark regions) in the 2D structure of BN confirms the attachment of the hydrophilic groups (OH and NH_2) at the edges of the AH-BN sheets (Fig. 6 (a)). The lattice arrangement of the AH-BN sheets was revealed by

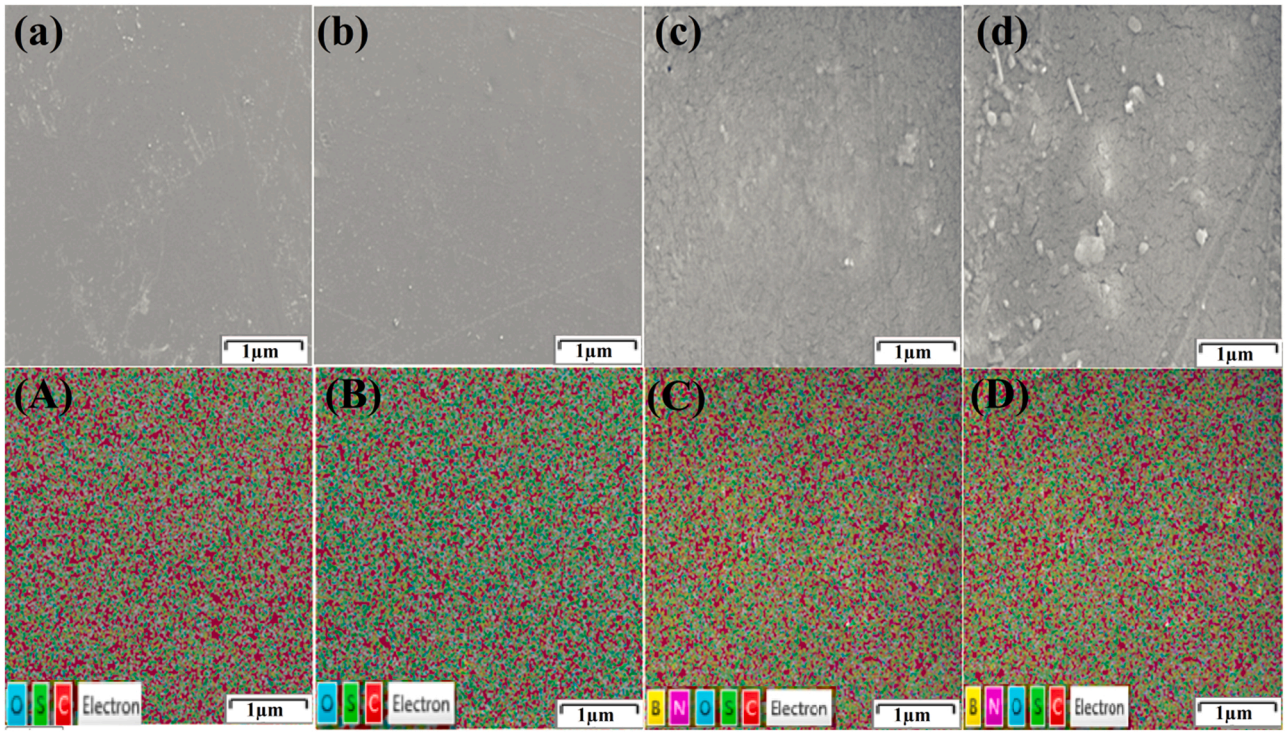

Fig. 4. FESEM of (a) SPEEK, (b) SR0, (c) SR2, (d) SR3 and mapping images of (A) SPEEK, (B) SR0, (C) SR2 (D) SR3.

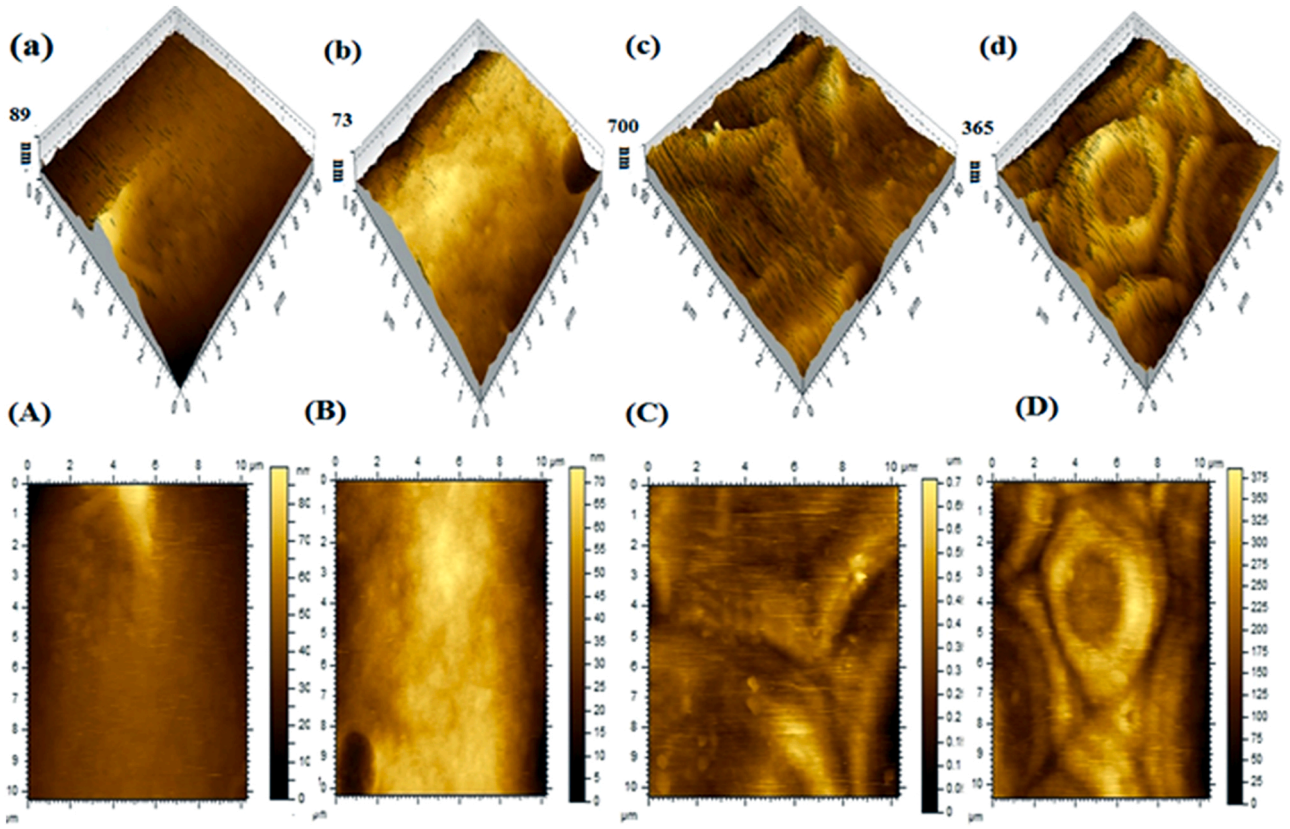

Fig. 5. AFM 3D images of (a) SPEEK, (b) SR0, (c) SR2, (d) SR3 and 2D images of (A) SPEEK, (B) SR0, (C) SR2, (D) SR3.

Table 1
The different roughness parameters of the prepared samples.

Membranes	Roughness parameters		
	Ra (nm)	Rq (nm)	Rz (nm)
SPEEK	3.01	3.96	20.1
SR0	2.64	3.46	18.3
SR2	9.48	13.3	70.7
SR3	5.96	7.49	37.5

HRTEM image and identified the exfoliated sheets with thickness of 5–6 layers are stacked in the lattice distance of 0.344 nm (Fig. 6(c)). The SAED pattern determined the individual layer distance through measuring the fringe diameter (0.356 nm), which belongs to the miller indices plane (002). These arguments confirm the layered 2D structure of AH-BN is arranged like a hexagonal atomic configuration (Fig. 6(b)) [25,34].

3.7. XPS

The XPS spectrum of the AH-BN sheets are shown in the Fig.S6, which confirmed the exfoliation, hydroxylation and functionlization of bulk BN. Fig.S6(a) displays the binding energies spectra at 189.2 eV and 190. 0 eV associated to the B-N and O-B bonding states. These verify the formation of H-BN sheets from the bulk BN via exfoliation and hydroxylation. The various peaks at 530.5 eV, 532.2 eV and 531.2 eV are assigned to the binding energy of O═C, O-C and HO-B bond, respectively. These shows the hydroxylation was occurred at the edges of exfoliated BN sheets in the boron atom via electrophilic substitution (π- π interaction) (Fig.S6 (b)) [35]. The C 1s shows the three prominent peaks at 283.6 eV, 285.1 eV, and 287.4 eV corresponds to C–C/C–H, C-O/C-N and C═O bond. The N ls core level exhibits the two spectra, one at 398.1 eV is assigned to the N-B bond and other at 400.1 eV is assigned to the N-H bond (NH_2) of the AH-BN (Fig.S6 (c)&(d)) [36,37]. The explanation correlates the formation of AH-BN sheets from the H-BN via hydrolysis and condensation process. The elevated ratio of the carbon in the AH-BN is the outcome of residual hydrocarbon and unreacted polydopamine (Table2).

3.8. TGA and DSC

The TGA gives the information about the thermal stability of the SPEEK composite membrane by the effect of the incorporated PES and AH-BN sheets (Fig. 7(a)). The three different weight losses are occurred at 170 °C, 210–380 °C and above 410 °C, which associated to the elimination of bound water molecules, sulfonic acids and the aromatic main chains from the polymer membrane. The exhibited weight losses in the three stages of SR2 membrane (7.7%, 19.43% and 22.34%) are lower compared to the SPEEK (10.56%, 37.67% and 40.34%). Its degradation temperatures in the each stage (196 °C, 242 °C and 461 °C) are improved than SPEEK with increment of 26, 32 and 51 °C, respectively [17,38]. The high thermal stability of SR2 membrane is facilitated by the combined effect of inherent thermal stability of AH-BN sheets and PES (sulfone backbone) via strong synergistic effect with SPEEK. The few layers AH-BN sheets possess the amine groups which facilitates the uniform dispersion and induced the strong interaction with the sulfonic acids via acid-base pairs ($^{-}$S-O–···$^{+}$H-N =) and forming the interpenetrating networks. These interconnecting polymer matrixes created the rigid polymer matrices that inhibit the thermal decomposition of the polymer chain finally minimized the weight loss. The weight loss of SR2 membrane at 170 °C is 93.34% it is crucial for the PEM application.

The glass transition (T_g) temperature of the SPEEK, SR0, SR2 and SR3 membrane were studied by the DSC technique. The combination of PES (20 wt%) with the high quantity of AH-BN sheets (4.5 wt%) in the SPEEK matrix highly improved the glass transition temperature from 73 °C to 102 °C, which is 29 °C higher than the SPEEK (73 °C) (Fig. 7(b)).

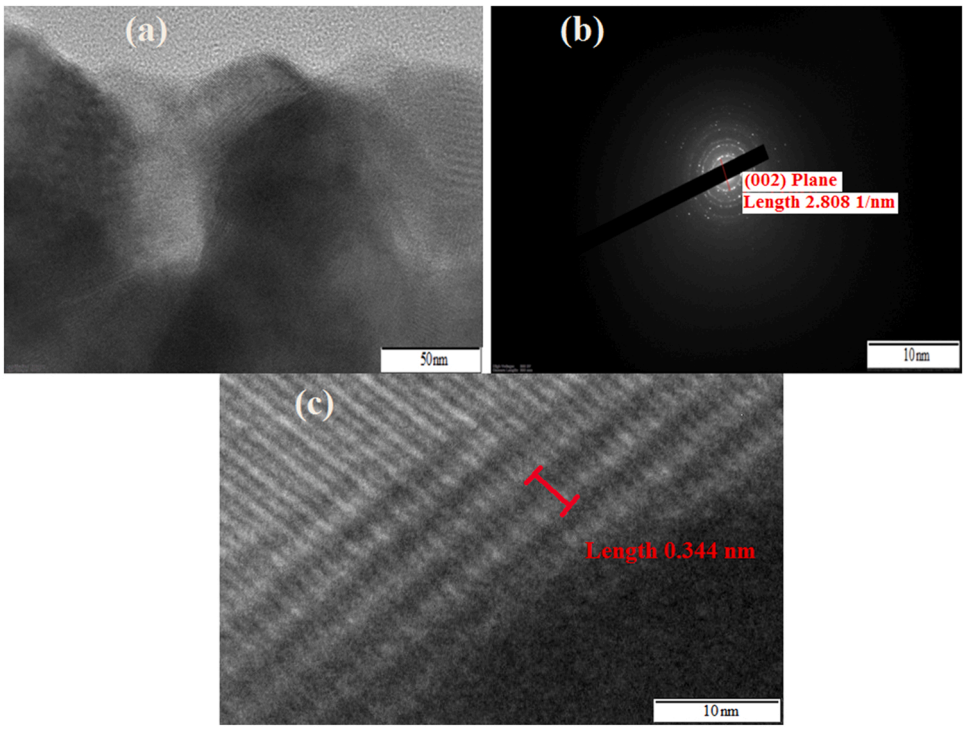

Fig. 6. (a) TEM, (b) SAED and (c) HRTEM image for AH-BN.

Table 2
XPS elemental quantification of AH-BN.

	Elemental composition (%)			
Sample Code	O (1s)	B (1s)	C (1s)	N (1s)
AH-BN	19.7	13.4	53	13.9

The sulfone in the PES and amine on AH-BN sheets are strongly interacted with the sulfonic acids of the SPEEK at the polymer-fillers interfaces formed the cross linked networks. These impeded the dispersion of crystalline domains in the amorphous regions and hinder the translation of polymer chain. The amines and hydroxyl are occupied at the edges of AH-BN sheets causes the lesser interfacial contact between the sheets produced the uniform dispersion and leads to the formation of less crystallized matrices [10]. The chain motion and transition temperature are mutually related to each other as the outcome T_g values was enhanced [39,40]. The ionic interaction of PES and AH-BN sheets with SPEEK matrix greatly hinder the re-orientation of crystalline domains and reduce the crystallinity of the polymer matrices.

3.9. Mechanical and oxidative

The tensile strength (T_s), young modules (Y_m) and the elongation at break (E_b) of the prepared membrane are measured against the external stress are shown in Fig. 8(a)&(b). The SR2 membrane contain the SPEEK (80 wt%) with addition to PES (20 wt%) and AH-BN (4.5 wt%) gives the highest value of T_s (22 MPa), Y_m (1278 MPa) and the lowest value of E_b (1.17%). The obtained value is ~7.23, 3.55 times higher and 5.62 times lower than SPEEK (Fig. 8(a)&(b)). The mechanical strength was maximized in the SR2 composite membrane by utilized the inherent mechanical strength of PES and AH-BN sheets [17,38,41]. In meticulous, high dispersion ability of the AH-BN sheets in the SPEEK-PES matrices causes the large synergy interfacial interplay with the sulfonic acids of SPEEK and transfer the excellent mechanical strength of the AH-BN to the composite membrane effectively. These synergy mechanisms change the SPEEK composite from the ductile to brittle nature [38].

The oxidative stability describes the durability and degradation of the membranes in the electrochemical study. The SR2 membrane shows the residual weight of 97.1 wt% after the 5 h of the exposure in the

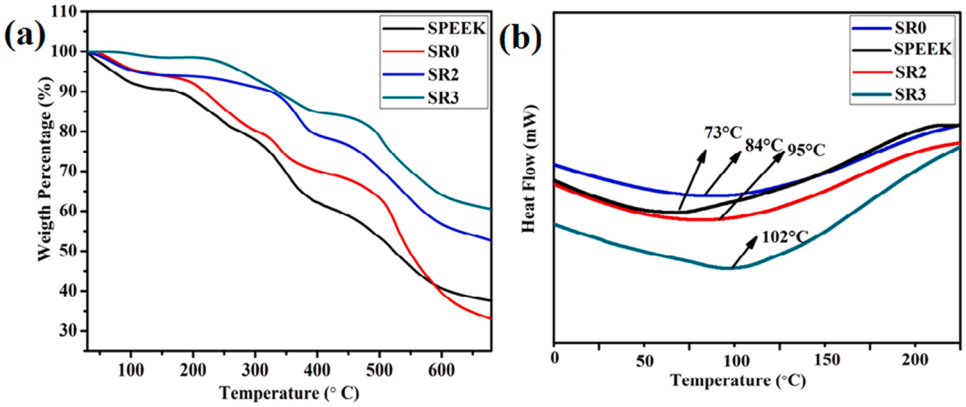

Fig. 7. (a) TGA and (b) DSC study for SPEEK, SR0, SR2 and SR3 membrane.

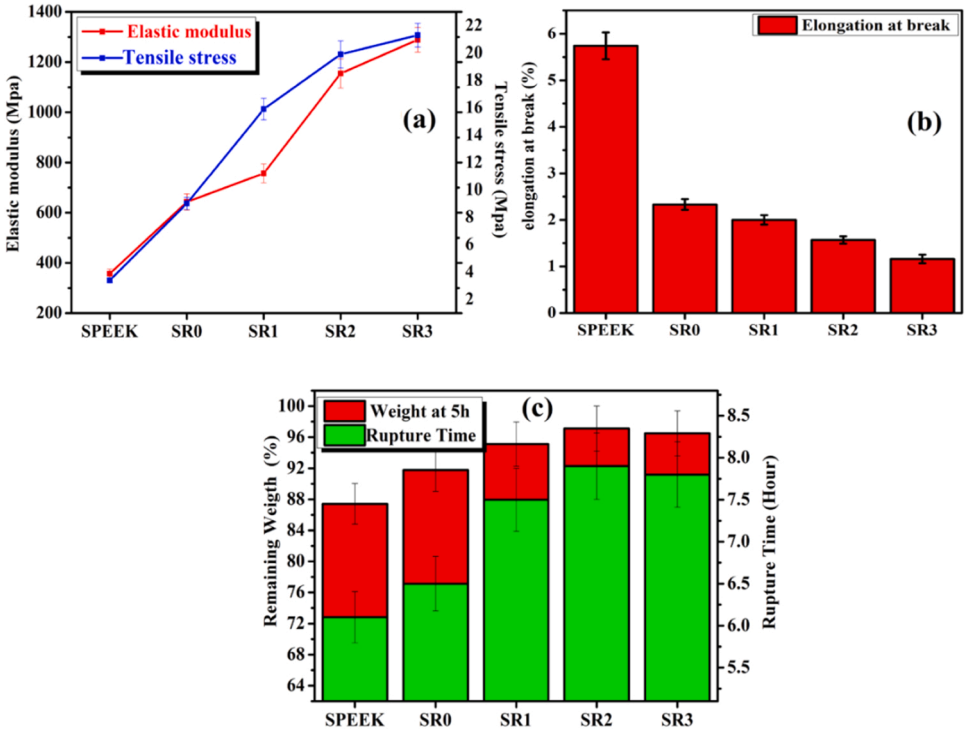

Fig. 8. (a) Tensile stress and elastic modulus, (b) elongation at break and (c) oxidative stability for SPEEK, SR0, SR1, SR2 and SR3 membrane.

Fenton solution this is higher than other membranes (Fig. 8(c)). This indicates the little impact of free radicals in the composite membranes in the effect of PES and AH-BN sheets in the SPEEK, which protects the sulfonic acids from the free radicals attack (Fig.S7(a)) [17,38]. The large interfacial interplay was created between the sulfonic acids and amine groups (–S-O$^{-}\cdots^{+}$H-HN–) in the composite matrix hinder the dissociation of HSO_3 groups in the SPEEK backbone. The loading of AH-BN sheets (3 wt%) in the SPEEK-PES matrix enhance the oxidative stability of the composite membranes. Fig.S7(b) shows the images of degradation of the membranes in the Fenton test after the sufficient time.

3.10. IEC, water uptake, swelling, hydration number and hydrolytic stability

The ion exchange capacity (IEC) identify the density of the functional groups (HSO_3) is ready to dissociate the protons (H^+) and exchange with the Na^+ ions. When added the PES (20 wt%) to the SPEEK the IEC value of the SR0 membrane was decreased from 1.65 to 1.62 meq g^{-1}. This is due to the ionic interplay between PES and SPEEK via sulfone (S═O) and sulfonic acids (HSO_3) restricted the exchange of protons (H^+). The SR1 membrane enhanced the IEC value from 1.62 to 1.67 meq g^{-1} and maximized to 1.72 meq g^{-1} for SR2 membrane is shown in Table3. The addition of AH-BN sheets (1.5, 3 & 4.5 wt%) to the SPEEK-PES matrix enhance the proton exchange process with the help of hydroxyl and the water molecules groups. After the addition of 4.5 wt% AH-BN sheets into the SPEEK-PES matrix aggregation effect was appeared in the composite matrix, which decreases the IEC value from 1.72 to 1.70 meq g^{-1} [40,42,43]. It is showed that the IEC of the composite membranes is higher than SPEEK and Nafion 117 (Table3). The water uptake and the swelling ratio determined the proton conductivity and stability of the membranes. The physical interaction between PES and SPEEK bridging the sulfone (S═O) with sulfonic acids (HSO_3) through hydrogen bond eliminates the water molecule clusters around the sulfonic acids, constructed the rigid interconnecting polymer matrices. Consequently decreases the water uptake (16.8% at 40 °C) and swelling ratio (26.6%) of SR0 membrane as compared to SPEEK (28.5 & 34.5%) (Fig. 9(a)&(b)). The SR2 membrane achieved the highest water uptake (56.7% at 80 °C) and lowest swelling ratio (27.5%) in the effect of the impregnation of AH-BN sheets in the SPEEK-PES matrix (Fig. 9(a)&(b)) [17,40,42]. The composite matrix constructs the more rigid structure in the effect of the physical interaction between the AH-BN sheets and SPEEK via acid-base interplay. The bearing of amines and hydroxyl

Table 3
The various properties of the polymer membranes.

Membrane	IEC (meq g^{-1})	(H_2O/SO_3H) (%)	Water uptake (%)	σ (mS cm^{-1})	E_a (kJ mol^{-1})	Swelling ratio (%)	hydrolytic stability wt%
SPEEK	1.65 ± 0.01	14.8 ± 0.3	44 ± 2.2	21.2 ± 0.9	17.5 ± 0.3	47.4 ± 2.3	82.7 ± 1.3
SR0	1.62 ± 0.01	8.56 ± 0.3	25.3 ± 1.2	14.8 ± 0.8	47.5 ± 0.4	36.5 ± 1.8	86.3 ± 0.7
SR1	1.67 ± 0.01	16.7 ± 0.3	50.4 ± 2.5	45.7 ± 1.1	15.6 ± 0.5	32.4 ± 1.6	89.1 ± 0.9
SR2	1.72 ± 0.01	18.3 ± 0.3	56.7 ± 2.8	79.8 ± 1.1	14.0 ± 0.5	27.5 ± 1.3	95.8 ± 0.7
SR3	1.70 ± 0.01	17.7 ± 0.3	54.4 ± 2.7	68.3 ± 0.9	15.0 ± 0.5	31.5 ± 1.5	93.8 ± 0.8
Nafion117	0.91 ± 0.01	19.2 ± 0.2	32.5 ± 0.9	63.2 ± 0.6	14.1 ± 0.4	25.1 ± 0.9-	–
SPEEK/GO-5	1.57	–	21.6	43.34	–	22.1	51[a]
SPEEK/SGO-5	1.64	–	26.3	46.54	16.18	25.3	51[a]
SPEEK/SSGO-5	1.66	–	30.1	53.35	15.61	27.4	51[a]
GO-g-SPEEK	1.27	37	85.3	21.23	0.159	20.6	32[a]
SPEEK-DGO-10	1.41	–	–	27.34	–	–	24[a]

a- reference number.

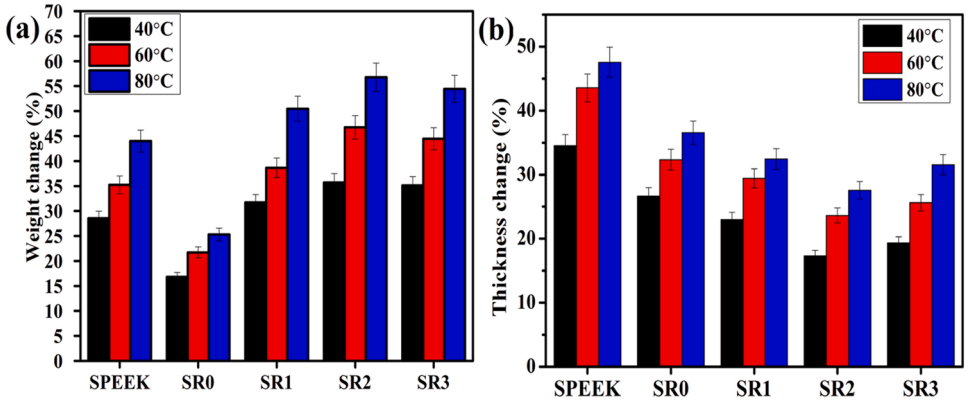

Fig. 9. (a) Water uptake and (b) swelling ratio for SPEEK, SR0, SR1, SR2 and SR3 membrane.

groups on the AH-BN sheets adsorbed the more water molecules, which interconnected the nano phase polymer separation and created the continuous interconnected ionic channels. In addition to this, the good dispersion ability of the 2D sheets helps to increases the ionic cluster channels between the hydrophobic polymer regions. The value of water uptake at this condition is higher than Nafion 117, whereas the swelling ratio is approximately equal. The aggregation effect was induced in the SR3 composite membrane due to weak acid-base interplay between the SPEEK and AH-BN in the results of the poor dispersion ability of 4.5 wt% AH-BN sheets. The water uptake and the swelling ratio are enhanced with respect to raise in the temperatures (30 °C to 80 °C) due to the vibration of the polymer domains, which enhanced the free volume space for the occupation of more water molecules. The bound water molecules in the polymer matrices can be calculated from the hydration number (λ) (Table3).

The numbers of bound water molecules around the sulfonic acids of SR2 membrane (18.3%) is higher compared to other membrane in the outcome of higher water uptake values, whereas less value was exhibited by the commercial Nafion 117 membrane (19.2%). The SR2 membrane achieved the maximum residual weight of 95.8 wt% after the hydrolytic study. The ionic interaction between the AH-BN, PES and SPEEK protect the sulfonic acids from the interaction of water molecules and restrict the dissociation of sulfonic acids. But, SPEEK membrane interacted directly with water molecules and initiated the degradation of the sulfonic acids in the polymer chain this causes the lowest remaining weight of 82.7 wt%.

3.11. Proton conductivity

The incorporation of PES and AH-BN sheets with SPEEK membrane significantly changes the proton conductivity and Arrhenius behavior are shown in Fig. 10(a)&(b). The analysis is conducted at temperatures from 30 °C to 80 °C in 50%RH condition to understand the acid-base proton migration mechanism. The SPEEK acquired the conductivity of 6.53 mS cm^{-1} at 30 °C owed to the facile transport of protons via sulfonic acids groups and water mediated ionic channels (Fig. 10(a)). The thermal disturbance causes the occupation of the water channels in the polymer matrix increases the conductivity to 21.2 mS cm^{-1} at 80 °C via vehicular mechanism [32]. The addition of PES to SPEEK arouse the electrostatic interaction between the sulfone (S═O) and sulfonic acid groups (HSO_3), which hinder the occupation of water channels in the polymer matrix and reduced the transport of the protons (H^+). As results, the conductivity is decreases from 6.53 to 1.53 mS cm^{-1} at 30 °C and from 21.2 to 14.8 mS cm^{-1} at 80 °C [44]. The Nafion 117 exhibited the conductivity of 24.3 mS cm^{-1} at 30 °C and improved to 63.2 mS cm^{-1} at 80 °C. The addition of AH-BN sheets (1.5, 3 and 4.5 wt%) into the SPEEK-PES raises the conductivity value of the composite membrane through the proton transfer mechanism such as Grotthuss and vehicular type. The conductivity of SR1 membrane is increases from 1.53 mS cm^{-1} to 23.4 mS cm^{-1} at 30 °C and 14.8–45.7 mS cm^{-1} at 80 °C (Fig. 10 (a)) [45,46]. This enhanced conductivity attributes the role of the AH-BN sheets in the proton transport mechanism. First, bearing of amine and hydroxyl groups at AH-BN sheets and its large surface area created the active sites for the transport of protons through the bound ionic clusters via dissociation mode.

Second, the created acid-base pairs (HSO_3– NH_2) at SPEEK and AH-BN interfaces provided the long-range conduction path via adsorption mode. The electrostatic interplay between the acid and base pairs act as proton donors (–$^+$HSO$^-$/$^+$H-HN–) and acceptors ($^+$H-N =), which conduct the protons via Grotthuss mechanism instead of formation of quaternary ammonium. The large pores size and the less potential barrier at the center of hexagonal rings favor the vehicular mechanism as

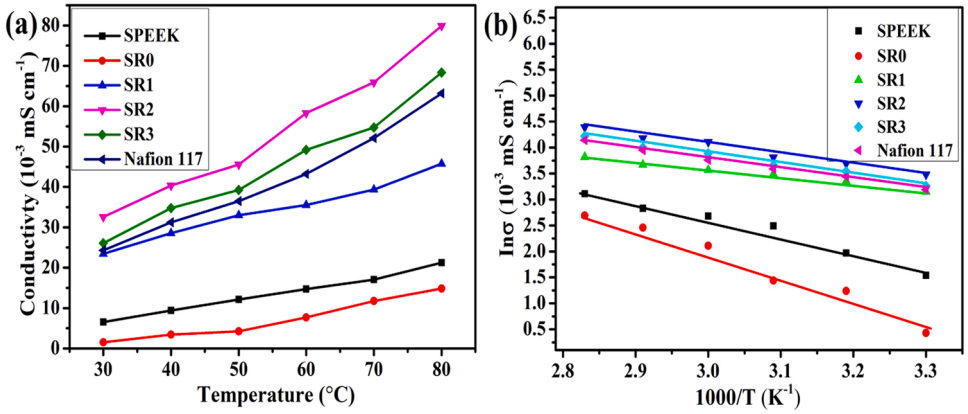

Fig. 10. (a) Proton conductivity and (b) Arrhenius behavior for SPEEK, SR0, SR1, SR2, SR3 and Nafion 117 membrane.

results in the interaction of the high negativity protons (H_3O^+) with the positive boron atoms (B^+) [47]. The SR2 membrane shows the proton conductivity of 79.8 mS cm^{-1} at 80 °C that is higher than Nafion 117 (63.2 mS cm^{-1}), where SR3 exhibits the decreases of conductivity (68.3 mS cm^{-1}) in the effect of poor dispersion ability of the 4.5 wt% AH-BN sheets [17,24,40]. The Grotthuss and vehicular type helps the transport of the protons, which lower the potential barrier and decreased the activation energy (E_a=14 kj mol^{-1}) of SR2 composite membrane (Fig. 10 (b)).

3.12. Fuel cell and durability

In view of excellent proton conductivity and the thermo-mechanical stability, the composite membrane with 3 wt% AH-BN is preferred for the study of fuel cell performance at 80 °C with the different relative humidified condition (50% and 75%RH) (Fig. 11(a)&(b)). The performance of SPEEK, SR0 and SR2 membrane is studied by the single cell type at 80 °C in the 50RH%. The obtained open circuit voltage (OCV) of the SPEEK is about 0.89 V signifies the inherent narrow polymer microstructure this restricted the gas crossover in the polymer matrix.

The SR0 membrane exhibits the high OCV of 0.89 V, but decreases the current and power density (279.12 mA cm^{-2} & 63.23 mA cm^{-2}) as compared to SPEEK (319.12 mA cm^{-2} & 74.23 mA cm^{-2}). The ionic interaction between the SPEEK and PES polymer via functional groups (···$^+$H-O-S- and –S═O^-···) affords the barrier networks and constrained the transport of the fuel and protons. As results, the degradation of the membrane is lesser due to the limited free radicals attack and increases the chemical stability of the polymer structure. By contrast, the performance of the SR2 composite membrane at 50%RH is 51% higher in the current density (621.6 mA cm^{-2}) and 56% enhanced in the power density (131.1 mW cm^{-2}) as compared to SPEEK. The PES and AH-BN sheets in the SPEEK block the hydrogen crossover across the electrolyte region; in addition to this the 2D structure also provides the large barrier against fuel transport this further prevents the formation of radicals. The arranged acid-base pairs (HSO_3-NH_2) at the SPEEK-PES and AH-BN interfaces induced the excellent compatibility in the interfacial of electrode-electrolyte regions, which in turn created the lesser electrolyte resistance and induced the easy movements of protons [48,49]. Besides, the reduction reaction at the cathode site was enhanced, which further improved the proton transporting ability and it is responsible for increases the voltage-current (V-I) relationship in the SR2 composite membrane [40,46,49]. The SR2 composite membrane is subjected to test the performance at 80 °C under the 75% of humidified condition to measure the effect of the hydrophilic condition on OCV and power density. As results, the current and the power density value is enhanced to 756 mA cm^{-2} and 172 mW cm^{-2}, respectively (Fig. 11b). Especially, the obtained OCV (0.98 V) is nearer to the cell potential of Nafion 117 and the power density value is higher than 142 mW cm^{-2}. The higher retention of water molecules aids the better performance due to the increase the back water diffusion from anode to cathode and retains the wet ability for the longer times. These reduced the ohmic resistance and enhance the proton transport mechanism.

Clearly, SR2 offers the notable proton transport membrane for PEM for operating at 80 °C with the different hydrous condition (50% and 75%RH). The results are included in the Table4 and compared with Nafion 115 and the other membranes. A PEMFC with SPEEK-PES/AH-BN (3 wt%) were subjected to test the durability to study long term stability (Fig. 12). It is shows that SPEEK-PES/AH-BN (3 wt%) exhibits an OCV degradation about 0.05 V at 80 °C with 75%RH after the 80 h of durability study. The less OCV degradation of SPEEK-PES/AH-BN (3 wt %) indicates that the small effect of the hydroperoxyl (HOO•) and hydroxyl (HO•) radicals in the SPEEK-PES/AH-BN (3 wt%).

This membrane established the retarded degradation owing to insufficient generation of the radicals in this system. The voltage retention of SPEEK-PES/AH-BN (3 wt%) is 0.87 V which is excellent in this conditions. The higher stability could be described the good compatibility effect of amphiphilic AH-BN with SPEEK-PES domains by strong interplay between the AH-BN and SPEEK via –NH_2 and –SO_3H groups.

4. Conclusion

The present study describes the use of AH-BN as an active 2D filler to prepare the improved conductive composites membranes for PEM fuel cells. The inclusion of AH-BN and PES enhance the thermal and mechanical stability of the SPEEK through the modification of nanophase structure and chain arrangement. The sulfonic acid in the SPEEK and –NH_2/–NH– in the AH-BN sheets are accumulated the acid–base pairs at

Table 4
Comparative study of SR2 sample with other membranes.

Membrane	Temperature (°C)	Max.Power density (mW cm^{-2})	Max. Current density (mA cm^{-2})	Reference
SR2	80	172	756	Present work
Nafion 117	80	142	557	Present work
SP-DSi	55	111.7	323.4	[10]
SPEEK/SSGO	120	119.6	403.3	[51]
SPEEK/GO-5	120	96.7	395.9	[51]
MSAIT1	80	123	515	[50]
SPEEK/ACNT	60	140.3	313.7	[15]
Nafion 115	60	114.6	54	[15]
GO-g-SPEEK	60	139	750	[32]
GO-g-SPEEK/ s-PBI-3	25	80.7	300	[32]
GO-g-SPEEK/ s- PBI-8	25	67	200	[32]

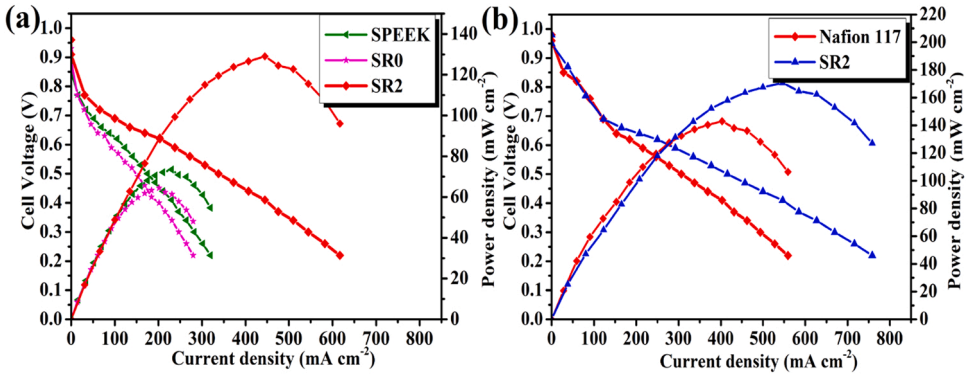

Fig. 11. Fuel cell study of (a) SPEEK, SR0, and SR2 membrane at 50RH% and (b) SR2 and Nafion117 membrane at 75RH%.

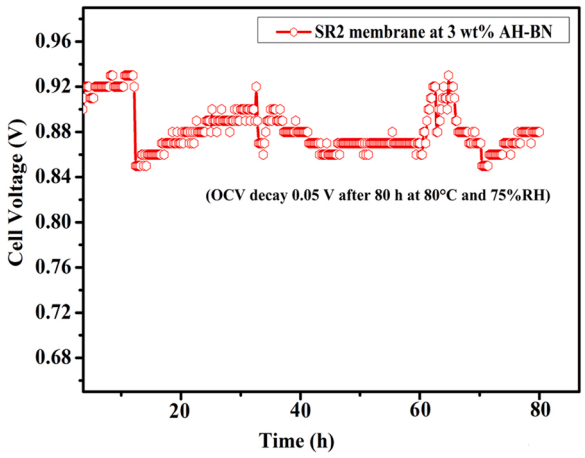

Fig. 12. Durability study of SR2 membrane.

the polymer-AH-BN interfaces; in that proton donor and acceptor are intimately connected, permits to perform the Grotthuss proton transport. As an effect, the enhanced conductivity (79.8 mS cm^{-1}) and cell performances (131.1 mW cm^{-2}) was obtained at 80 °C in the 50%RH by the composite membrane (SR2) due to the assembly of low resistance barrier pathways using the acid–base scheme. This membrane achieved the highest OCV (0.98 V), power density (172 mW cm^{-2}) and the excellent durability at 80 °C with the 75%RH after the 80 h of accelerated stability test. The chemical, mechanical, oxidative and the water uptake parameters are described herein may cover the understanding mechanism of the acid–base pairs in the composites membrane for usage in the fuel cell device.

CRediT authorship contribution statement

Raja Pugalenthi M: Conceptualization, Methodology, Writing – original draft, Writing – review & editing, **Gayathri R:** Data curation, Software and Validation. **Guozhong Cao:** Visualization and Investigation. **Ramesh Prabhu M:** Supervision.

Declaration of Competing Interest

The authors declare that they have no known competing financial interests or personal relationships that could have appeared to influence the work reported in this paper.

Acknowledgements

The authors acknowledge the DST- Science and Engineering Research Board (SERB NO: EEQ/2017/000033) and RUSA 2.0, Govt. of India for their financial support and also thank the UGC-SAP DRS III, DST-FIST, DST-PURSUE for providing the characterization facilities in Alagappa university.

Appendix A. Supporting information

Supplementary data associated with this article can be found in the online version at doi:10.1016/j.jece.2021.107025.

References

[1] S. Sharma, B.G. Pollet, Support materials for PEMFC and DMFC electro catalysts-a review, J. Power Sources 208 (2012) 96–119.
[2] M.Z. Jacobson, W.G. Colella, D.M. Golden, Cleaning the air and improving health with hydrogen fuel-cell vehicles, Science 308 (2005) 1901–1905.
[3] N. Üregen, K. Pehlivanoğlu, Y. Özdemir, Y. Devrim, Development of polybenzimidazole/graphene oxide composite membranes for high-temperature PEM fuel cells, Int. J. Hydrog. Energy 42 (2017) 2636–2647.
[4] N. Zhang, B. Wang, Y. Zhang, F. Bu, Y. Cui, X. Li, C. Zhao, H. Na, Mechanically reinforced phosphoric acid doped quaternized poly(ether ether ketone) membranes via cross-linking with functionalized graphene oxide, Chem. Commun. 50 (2014) 15381–15384.
[5] A. Iulianelli, A. Basile, Sulfonated PEEK-based polymers in PEMFC and DMFC applications: a review, Int. J. Hydrog. Energy 37 (2012) 15241–15255.
[6] S. Gahlot, H. Gupta, P.K. Jha, V. Kulshrestha, Enhanced electrochemical performance of stable SPES/SPANI composite polymer electrolyte membranes by enriched ionic nanochannels, ACS Omega 2 (2017) 5831–5839.
[7] L.Y. Li, B.C. Yu, C.M. Shih, S.J. Lue, Polybenzimidazole membranes for direct methanol fuel cell: acid-doped or alkali-doped? J. Power Sources 287 (2015) 386–395.
[8] A. Muthumeenal, S. Neelakandan, P. Kanagaraja, A. Nagendrana, D. Ranab, T. Matsuura, Enhancing proton conduction of sulfonated poly (phenylene ether ether sulfone) membrane by charged surface modifying macromolecules for H_2/O_2 fuel cells, Renew. Energy 78 (2015) 306–313.
[9] D. Martınez-Casillas, O. Solorza, S. Molla, A. Montero, A. Garcıa-Bernabe, V. Compa, Polymer modified sulfonated PEEK ionomers membranes and the use of Ru_3Pd_6Pt as cathode catalyst for H_2/O_2 fuel cells, Int. J. Hydrog. Energy 44 (2019) 295–303.
[10] J. Wang, H. Bai, H. Zhang, L. Zhao, H. Chen, Y. Li, Anhydrous proton exchange membrane of sulfonated poly(ether ether ketone) enabled by polydopamine modified silica nanoparticles, Electrochim. Acta 152 (2015) 443–455.
[11] L.G. Trindade, E.C. Pereira, SPEEK/Zeolite/Ionic-Liquid anhydrous polymer membranes for fuel-cell applications, Eur. J. Inorg. Chem. 17 (2017) 2369–2376.
[12] M.M. Hasani-Sadrabadia, E. Dashtimoghadama, K. Sarikhania, F.S. Majedi, G. Khanbabaei, Electrochemical investigation of sulfonated poly(ether ether ketone)/clay nanocomposite membranes for moderate temperature fuel cell applications, J. Power Sources 195 (2010) 2450–2456.
[13] Z. Zhao, C. Pan, L. Xue, G. Jiang, M. Zhong, B. Fei, Electrochemical properties of SPEEK/epoxy semi-interpenetrating network composites as proton exchange membrane, Int. J. Electrochem. Sci. 13 (2018) 925–935.
[14] Y. Huanga, T. Chenga, X. Zhanga, W. Zhang, X. Liu, Novel composite proton exchange membrane with long-range proton transfer channels constructed by synergistic effect between acid and base functionalized graphene oxide, Polymer 149 (2018) 305–315.
[15] A.R. Kim, M. Vinothkannan, M.H. Song, J.-Y. Lee, H.-K. Lee, D.J. Yoo, Amine functionalized carbon nanotube (ACNT) filled in sulfonated poly(ether ether ketone) membrane: Effects of ACNT in improving polymer electrolyte fuel cell performance under reduced relative humidity, Compos. Part B Eng. 188 (2020), 107890.
[16] H.-L. Wu, C.-C.M. Ma, F.-Y. Liu, C.-Y. Chen, S.-J. Lee, C.-L. Chiang, Preparation and characterization of poly(ether sulfone)/sulfonated poly(ether ether ketone) blend membranes, Eur. Polym. J. 42 (2006) 1688–1695.
[17] S.H. Hong, J.-K. Park, J.W. Choi, Enhanced durability of polymer electrolyte membrane fuel cells by functionalized 2D boron nitride nanoflakes, ACS Appl. Mater. Interfaces 6 (2014) 7751–7758.
[18] V. Yadava, V. Kulshrestha, Boron nitride: a promising material for proton exchange membranes for energy applications, Nanoscale 11 (2019) 12755–12773.
[19] S.I. Yoon, K.Y. Ma, T.-Y. Kimb, H.S. Shin, Proton conductivity of a hexagonal boron nitride membrane and its energy applications, J. Mater. Chem. A 8 (2020) 2898–2912.
[20] S. Hu, M.L. Hidalgo, F.C. Wang, A. Mishchenko, F. Schedin, R.R. Nair, E.W.D. Hill, W. Boukhvalov, M.I. Katsnelson, R.A.W. Dryfe, I.V. Grigorieva, H.A. Wu, A. K. Geim, Proton transport through one-atom-thick crystals, Nature 516 (2014), 227-23.
[21] D. Lee, S.H. Song, J. Hwang, S.H. Jin, K.H. Park, B.H. Kim, S.H. Hong, S. Jeon, Enhanced mechanical properties of epoxy nanocomposites by mixing noncovalently functionalized boron nitride nanoflakes, Small 9 (2013) 2602–2610.
[22] A. Yusuf, S.U. Celik, A. Bozkurt, Synthesis and anhydrous proton conductivity of doped azole functional PGMA-hBN nano-flakes, Synth. Met. 241 (2018) 1–6.
[23] T. Sainsbury, T. Ikuno, D. Okawa, D. Pacile, J.M.J. Frechet, A. Zettl, Self-assembly of gold nanoparticles at the surface of amine- and thiol-functionalized boron nitride nanotubes, J. Phys. Chem. C 111 (2007) 12992–12999.
[24] Y. He, J. Wang, H. Zhang, T. Zhang, B. Zhang, S. Cao, J. Liu, Polydopamine-modified graphene oxide nanocomposite membrane for proton exchange membrane fuel cell under anhydrous conditions, J. Mater. Chem. A. 2 (2014) 9548–9558.
[25] J. Liu, L. Yu, X. Cai, U. Khan, Z. Cai, J. Xi, B. Liu, F. Kang, Sandwiching h-BN monolayer films between sulfonated poly(ether ether ketone) and nafion for proton exchange membranes with improved ion selectivity, ACS Nano 13 (2019) 2094–2102.
[26] M. Raja Pugalenthi, C. Liu, G. Cao, R. Prabhu, Tailoring SPEEK/SPVdF-co-HFP/$La_2Zr_2O_7$ ternary composite membrane for cations exchange membrane fuel cells, Ind. Eng. Chem. Res. 59 (2020) 4881–4894.
[27] M.N. Ivanova, E.D. Grayfer, E.E. Plotnikova, L.S. Kibis, G. Darabdhara, P. K. Boruah, M.R. Das, V.E. Fedorov, Pt-decorated boron nitride nanosheets as artificial nanozyme for detection of dopamine, ACS Appl. Mater. Interfaces 11 (2019) 22102–22112.
[28] G. Mittal, K.Y. Rhee, S.J. Park, Processing and characterization of PMMA/PI composites reinforced with surface functionalized hexagonal boron nitride, Appl. Surf. Sci. 415 (2017) 49–54.
[29] Y. Shi, C. Hamsen, X. Jia, K.K. Kim, A. Reina, M. Hofmann, A.L. Hsu, K. Zhang, H. Li, Z.Y. Juang, M.S. Dresselhaus, L.J. Li, J. Kong, Synthesis of few-layer hexagonal boron nitride thin film by chemical vapor deposition, Nano Lett. 10 (2010) 4134–4139.

[30] D. Lee, S.H. Song, Ultra-thin ultraviolet cathodoluminescent device based on exfoliated hexagonal boron nitride, RSC Adv. 7 (2017) 7831–7835.
[31] H. Wu, X. Shen, T. Xu, W. Hou, Z. Jiang, Sulfonated poly(ether ether ketone)/amino-acid functionalized titania hybrid proton conductive membranes, J. Power Sources 213 (2012) 83–92.
[32] S. Gao, H. Xu, Z. Fang, A. Ouadah, H. Chen, X. Chen, L. Shi, B. Ma, C. Jing, C. Zhu, Highly sulfonated poly(ether ether ketone) grafted on graphene oxide as nanohybrid proton exchange membrane applied in fuel cells, Electrochim. Acta 283 (2018) 428–437.
[33] M. Akel, S.Ü. Çelik, A. Bozkurt, A. Ata, Nano hexagonal boron nitride–Nafion composite membranes for proton exchange membrane fuel cells, Polym. Compos. 37 (2016) 422–428.
[34] A.S. Nazarov, V.N. Demin, E.D. Grayfer, A.I. Bulavchenko, A.T. Arymbaeva, H.-J. Shin, J.-Y. Choi, V.E. Fedorov, Functionalization and dispersion of hexagonal boron nitride (h-BN) nanosheets treated with inorganic reagents, Chem. Asian J. 7 (2012) 554–560.
[35] G. Zhao, F. Zhang, Y. Wu, X. Hao, Z. Wang, X. Xu, One-step exfoliation and hydroxylation of boron nitride nanosheets with enhanced optical limiting performance, Adv. Opt. Mater. 4 (2016) 141–146.
[36] Y. Song, Y. Shen, H. Liu, Y. Lin, M. Li, C.-W. Nan, Enhanced dielectric and ferroelectric properties induced by dopamine-modified $BaTiO_3$ nanofibers inflexible poly(vinylidene fluoride-trifluoroethylene) nanocomposites, J. Mater. Chem. 22 (2012) 8063–8068.
[37] W. Jin, W. Zhang, Y. Gao, G. Liang, A. Gu, L. Yuan, Surface functionalization of hexagonal boron nitride and its effect on the structure and performance of composites, Appl. Surf. Sci. 270 (2013) 561–571.
[38] V. Yadav, A. Rajput, N.H. Rathod, V. Kulshresth, Enhancement in proton conductivity and methanol cross-over resistance by sulfonated boron nitride composite sulfonated poly (ether ether ketone) proton exchange membrane, Int. J. Hydrog. Energy 45 (2020) 17017–17028.
[39] S. Madakbaş, E. Çakmakçı, M.V. Kahraman, Preparation and thermal properties of polyacrylonitrile/hexagonal boron nitride composites, Thermochim. Acta 552 (2013) 1–4.
[40] H. Zhang, T. Zhang, J. Wang, F. Pei, Y. He, J. Liu, Enhanced proton conductivity of sulfonated poly (ether ether ketone) membrane embedded by dopamine-modified nanotubes for proton exchange membrane fuel cell, Fuel Cells 13 (2013) 1155–1165.
[41] S.Y. Yang, W.N. Lin, Y.L. Huang, H.W. Tien, J.Y. Wang, C.C.M. Ma, S.M. Li, Y. S. Wang, Synergetic effects of graphene platelets and carbon nanotubes on the mechanical and thermal properties of epoxy composites, Carbon 49 (2011) 793–803.
[42] Y. Yin, T. Xu, G. He, Z. Jiang, H. Wu, Fabrication of sulfonated poly(ether ether ketone)-based hybrid proton-conducting membranes containing carboxyl or amino acid functionalized titania by in situ, sole gel process, J. Power Sources 276 (2015) 271–278.
[43] W. Jia, P. Wu, Stable boron nitride nanocomposites based membranes for high-efficiency proton conduction, Electrochim. Acta 273 (2018) 162–169.
[44] S. Elakkiya, G. Arthanareeswaran, K. Venkatesh, J. Kweon, Enhancement of fuel cell properties in polyethersulfone and sulfonated poly (ether ether ketone) membranes using metal oxide nanoparticles for proton exchange membrane fuel cell, Int. J. Hydrog. Energy 43 (2018) 21750–21759.
[45] M. Akel, S.U. Celik, A. Bozkurt, A. Ata, Nano hexagonal boron nitride–nafion composite membranes for proton exchange membrane fuel cells, Polym. Compos. 37 (2014) 422–428.
[46] W. Jia, B. Tang, P. Wu, Novel composite proton exchange membrane with connected long-range ionic nanochannels constructed via exfoliated nafion - boron nitride nanocomposite, ACS Appl. Mater. Interfaces 9 (2017) 14791–14800.
[47] M. Seel, R. Pandey, Proton, hydrogen transport through two-dimensional monolayers, 2D Mater. 3 (2016), 025004.
[48] K.H. Oh, H.S. Kang, M.J. Choo, D.H. Jang, D. Lee, D.G. Lee, T.H. Kim, Y.T. Hong, J. K. Park, H.T. Kim, Interlocking membrane/catalyst layer interface for high mechanical robustness of hydrocarbon-membrane-based polymer electrolyte membrane fuel cells, Adv. Mater. 27 (2015) 2974–2980.
[49] G. Rambabu, S.D. Bhat, Amino acid functionalized grapheme oxide based nanocomposite membrane electrolytes for direct methanol fuel cells, J. Membr. Sci. 551 (2018) 1–11.
[50] P. Salarizadeh, M. Javanbakht, S. Pourmahdian, H. Beydaghi, Influence of amine-functionalized iron titanate as filler for improving conductivity and electro chemical properties of SPEEK nanocomposite membranes, Chem. Eng. J. 299 (2016) 320–331.
[51] L. Zhao, Y. Li, H. Zhang, W. Wu, J. Liu, J. Wang, Constructing proton-conductive highways within an ionomer membrane by embedding sulfonated polymer brush modified graphene oxide, J. Power Sources 286 (2015) 445–457.
[52] S.E. Hosseini, B. Butler, An overview of development and challenges in hydrogen powered vehicles, Int. J. Green Energy 17 (2020) 13–37.
[53] M. Balat, M. Balat, Political, economic and environmental impacts of biomass-based hydrogen, Int. J. Hydrog. Energy 34 (2009) 3589–3603.
[54] K. Zeng, D. Zhang, Recent progress in alkaline water electrolysis for hydrogen production and applications, Prog. Energy Combust. Sci. 36 (2010) 307–326.
[55] S. Kim, S.Y. Cho, K. Son, N.F. Attia, H. Oh, A metal-doped flexible porous carbon cloth for enhanced CO_2/CH_4 separation, Sep. Purif. Technol. 277 (2021), 119511.
[56] M. Jung, J. Park, S.Y. Cho, S.E.A. Elashery, N.F. Attia, H. Oh, Flexible carbon sieve based on nanoporous carbon cloth for efficient CO_2/CH_4 separation, Surf. Interfaces 23 (2021), 100960.
[57] K. Raja, M. Raja Pugalenthi, M. Ramesh Prabhu, Investigation on the sulfonated poly(ether etherketone)/poly(amide-imide)/barium cerate-based nanocomposite membrane for proton exchange membrane fuel cells, Int. J. Energy Res. 45 (6) (2021) 8564–8576.
[58] K. Raja, M. Raja Pugalenthi, M. Ramesh Prabhu, The effect of incorporation of ferrous titanate nanoparticles in sulfonated poly(ether ether ketone)/poly (amide imide) acid-base polymer for cations exchange membrane fuel cells, J. Solid State Electrochem. 24 (2020) 35–44.
[59] K. Raja, M. Raja Pugalenthi, M. Ramesh Prabhu, Investigation on SPEEK/PAI/$SrTiO_3$-based nanocomposite membrane for high-temperature proton exchange membrane fuel cells, Ionics 25 (11) (2019) 5177–5188.
[60] R. Gayathri, M.R. Prabhu, Protonated state and synergistic role of Nd^{3+} doped barium cerate perovskite for the enhancement of ionic pathways in novel sulfonated polyethersulfone for H_2/O_2 fuel cells, Soft Matter 16 (2020) 4220–4233.
[61] M. Raja Pugalenthi, G. Cao, M. Ramesh Prabhu, Cross-Linked SPEEK−PEG−APTEOS-modified $CaTiO_3$ perovskites for efficient acid−base cation-exchange membrane fuel cell, Energy Fuels 34 (8) (2020) 10087–10099.
[62] P. Martina, R. Gayathri, M. Raja Pugalenthi, G. Cao, C. Liu, M. Ramesh Prabhu, Nano-sulfonated silica incorporated SPEEK/S-PVdF-HFP polymer blend membrane for PEM fuel cell application, Ionics 26 (2020) 3447–3458.
[63] M.; Raja Pugalenthi, M. Ramesh Prabhu, The Pore filled SPEEK nanofibers matrix combined with ethylene diamine modified $SrFeO_3$ nanoneedles for the cation exchange membrane fuel cells, J. Taiwan Inst. Chem. Eng. 122 (2021) 136–147.
[64] M. Raja Pugalenthi, M. Ramesh Prabhu, Synergistic effect of polydopamine-modified $CaZrO_3$ perovskite and hydroxylated SPEEK on acid–base cation exchange membrane fuel cells, Energy Fuels 35 (20) (2021) 16837–16849.
[65] R.K. Gayathri, C. Guozhong, Ramesh, M. Prabhu, Sandwich assembly of sulfonated poly (ether sulfone) with sulfonated multiwalled carbon nanotubes as an efficient architecture for enhanced electrolyte performance in H_2/O_2 fuel cells, Int. J. Energy Res. (2021) 13.
[66] R.N. Karnik, Breakthrough for protons, Nature 516 (2014) 173–175.
[67] W. Meng, Y. Huang, Y. Fu, Z. Wang, C. Zhi, Polymer composites of boron nitride nanotubes and nanosheets, J. Mater. Chem. C 2 (2014) 10049–10061.